



NIKHEF-H/93-10

Simulation of frontend preamplifiers for the MSGC

J. Schmitz

NIKHEF-H, Amsterdam, The Netherlands

Abstract

Two candidate architectures for frontend preamplifiers for the Microstrip Gas Counter are tested using a Monte Carlo simulation of the detector and frontend. The simulation describes ionisation in the gas, electron drift and diffusion, gas amplification, signal development and the discriminator. The first architecture is based on the current design of the Fastplex, while the alternative design uses a subtraction method. The simulations indicate that the current Fastplex-design matches the MSGC best when the shaping time is as high as possible (around 50 ns). The signal is extracted more accurately with the alternative design.

1 Introduction

The Microstrip Gas Counter (MSGC) is a very thin gas-filled detector, used for the localisation of relativistic charged particles, and photons. It is based on the geometry and operation of a Multiwire Proportional Chamber (MWPC); to come to a higher granularity than the MWPC can reach, the MSGC has strips etched on an insulating substrate, instead of wires strung in a gas volume. This way the anode-to-anode distance can be decreased to $\sim 200 \mu\text{m}$, which leads to a very high rate capability ($> 1 \text{ MHz}/\text{cm}^2$) and good position resolution ($30\text{--}50 \mu\text{m}$). This makes the device a very interesting candidate for charged particle tracking in LHC and SSC experiments.

The geometry of the detector is shown in fig. 1. Particles are supposed to cross the detector vertically, i.e. perpendicular to the strip plane ($\theta = 0$ in the figure). The distance between the strip plane and the drift cathode, L , is a few mm. This dimension determines the duration of the signal on the strips, because it takes an electron tens of nanoseconds to drift through this gap, from the top towards one of the anodes.

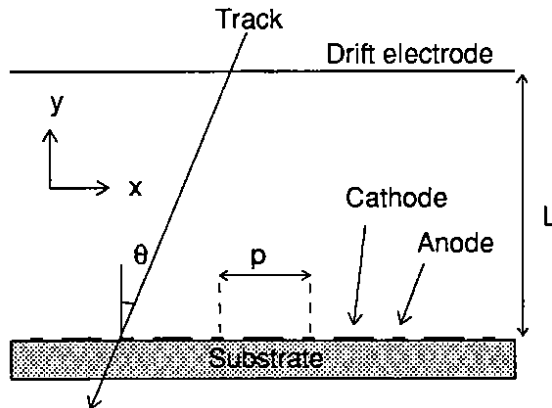


Figure 1: *Geometry of the MSGC.*

This paper describes the requirements on a fast frontend preamplifier for the MSGC strip readout. Essentially, with 'fast' we mean that the detector should have a minimal dead time on the scale set by the LHC bunch crossing period of 25 ns. In section 2, the simulation of the MSGC is briefly described. A more detailed description can be found in [1]. Section 3 deals with the different schemes proposed for the frontend preamplifier. The results are listed in section 4.

2 Description of the Monte Carlo simulation

A two-dimensional projection of the detector is used for simulating the MSGC (as in figure 1). A minimum ionising particle traveling through the detector causes a number of (primary) ionisations of gas molecules (typically 3–25 on a 3 mm track). Each primary electron (δ -electron) can in turn ionise more molecules, so the electrons are grouped in clusters. In

the simulation, these clusters are pointlike. They occur almost on the track of the crossing particle.

From their starting point, the liberated electrons will drift towards the strip plane with an average speed $\geq 50 \mu\text{m}/\text{ns}$. While drifting they undergo a displacement in x because of transverse diffusion. When the electrons reach the quadrupole field (close to the strips) they will be focused towards one of the anodes. Here the electric field is so high that gas amplification occurs: each electron will cause a shower in the gas, and more and more electrons are liberated. This way tens of thousands of electrons will reach the anode strips. This signal is in principle high enough to be detected with state-of-the-art electronics, with noise levels below 1500 equivalent noise charge (ENC).

The detector was described with the following parameters. The gas amplification factor was set to 2000, the drift velocity to $60 \mu\text{m}/\text{ns}$, the anode pitch to $230 \mu\text{m}$ and the gas gap to 3 mm. These numbers match the current design of the ATLAS MSGC detector. As a gas mixture we took DME/CO₂ 60/40. Each electron gives rise to a negative current pulse on an anode, with a fluctuating amplitude around 2000 electrons and a decay time constant of 3 ns.

In the simulation the signal development is followed step by step, where each step is around 0.3 ns. In this time bin the signal is assumed to be constant. Usually, most of the noise in a preamplifier is kT -noise at the input of the first preamplifier component. This white noise is approximated by adding a different Gaussian random number to the bare anode signal in each time bin. The noise is calibrated at the input to give the requested noise level at the preamplifier output. Before the particle crosses the detector, each channel is simulated over a period of 3 times the integrator decay time to randomise the low frequency component of the noise.

3 Two schemes for a fast frontend preamplifier

The MSGC is currently under study for inner tracking in experiments at the Large Hadron Collider (LHC). The high bunch crossing frequency (40 MHz) and high charged particle flux (1% hit probability on each channel) in these experiments call for fast preamplifiers, to have a recovery time of the order of 100 ns or less. Because the signal of an MSGC is spread out over a period of the order of 50 ns, a very fast preamplifier/shaper will tend to 'forget' the first part of the signal even before the last part has come in. This degrades the signal-to-noise ratio. The shaping time of the analog preamplifier of a frontend therefore needs careful optimisation to avoid signal loss in this very first stage of the signal processing.

In principle, this discussion deals with the signal-to-noise ratio of the MSGC together with the frontend preamplifier. But with a signal that is as highly fluctuating as the one from the MSGC, the *average* signal-to-noise does not tell us how often we lose a particle signal. We decided therefore to determine the probability that the signal of a crossing particle goes over threshold (the detector efficiency) for various preamplifier designs, because this is essentially the parameter we are interested in.

Two preamplifier schemes were simulated. At the time of the simulation, no information was available on the expected noise level of these preamplifiers, so this number was left as a

free parameter. Instead, we fixed the detector efficiency to 98%, which seems a reasonable aim (there will be other contributions to the overall detector inefficiency but the detector efficiency in this context is just the probability that if everything else works, a crossing particle will be detected by an MSGC monolayer). So all MSGC parameters are fixed, and we determine the maximum tolerable noise level of each preamplifier design. The two schemes simulated as MSGC frontends are shown in figure 2. (These schemes symbolise the implementation in the simulation, not the optimal implementation in reality.) The first scheme, labeled 'Fastplex-A', looks most like the current design of the Fastplex preamplifier [2]. The analog part of this chip

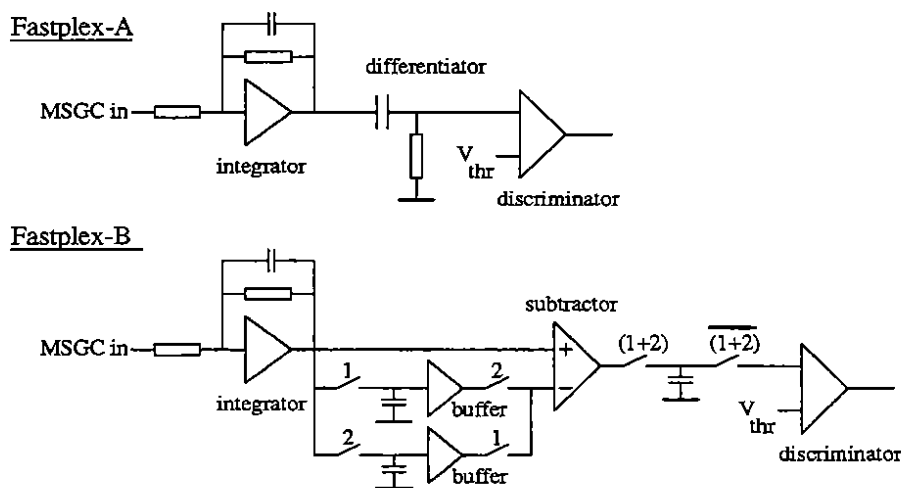


Figure 2: The two schemes compared in the simulation.

has a preamplifier/shaper with a peaking time around 15 ns and a shaping time constant of about 10 ns. It consists of an integrator/amplifier followed by a differentiating element. The shaping time (determined by the values of the resistors and capacitors) should be kept below around 50 ns, because the shaping time determines how long the signal will be over threshold and therefore the dead time of the detector. Two parameters determine the characteristic behaviour of the simulated shaper: the rise time (which is the time the signal needs to grow from 10% to 90% of the peak signal, in response to a test pulse), and the shaping time (the characteristic time of the integrator and differentiator). Both are determined by the values of the resistors and capacitors in the scheme. The discriminator is continuous, it will switch to 1 when the signal at the input goes over threshold and is reset at each bunch crossing clock signal. (A latched discriminator was also tried in the simulation but it combines very badly with the fast shaper, yielding much signal loss in case the shaping time is less than 40 ns.) In all simulation runs, the threshold was set to 5 times the noise level.

The second scheme ('Fastplex-B') is a bit more complex. It starts with a slow integrator (decay time of the order of $1 \mu s$). The rise time of this scheme will be around 20 ns. Two memory units (capacitors) behind the integrator store the signal every two bunch crossings, alternatingly. This signal is lead through to a subtractor two bunch crossings later, where it is compared to the signal at that time (see figure 3). This way the (latched) discriminator

behind the subtractor will switch to 1 when the current integrator output is much higher than the signal two bunch crossings before. (The comparison is made over 2 bunch crossings

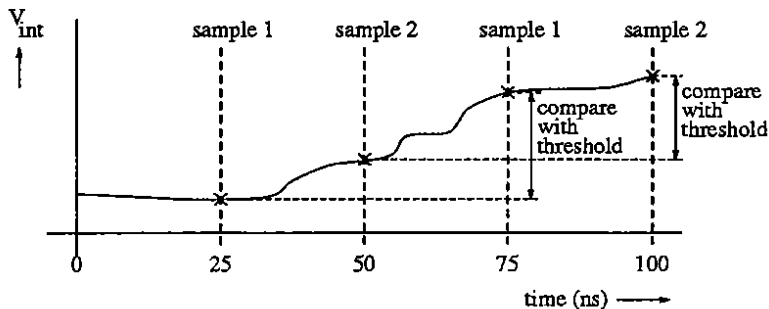


Figure 3: Signal processing of the Fastplex-B behind the integrator. The integrated signal is stored each 25 ns. The discriminator always compares signals between samples that are two bunch crossings apart.

(50 ns) because the signal of the MSGC will have a similar duration.) The slower integrator gives a better stacking of the signals from the individual ionisation clusters, so this scheme will yield a higher signal than the Fastplex-A. On the other hand, the switches may add to the noise figure, depending on the hardware implementation.

In the simulation, the integration of the signal is approximated by a summation. The signal is divided into time bins of one time unit t ; the 'integral' at time T is given by

$$I(T) = \sum_{t=0}^{t=T} S_t (e^{-t/\tau_{int}} - e^{-t/\tau_{rise}}) \quad (1)$$

Here, S_t is the signal at time t , and τ_{rise} is the characteristic time constant that determines the rise time. It is not the rise time itself, because this parameter is (here) defined as the time in which the integrator output rises from 10% to 90% of the maximum signal, in response to a test pulse. Although in real life τ_{rise} and τ_{int} are not independent, they are varied separately in the Monte Carlo.

The differentiation (in case A) is described by the weighted differential sum

$$D(T) = \sum_{t=0}^{t=T} (I_t - I_{t-1}) e^{-t/\tau_{dif}} \quad (2)$$

The differentiation causes an undershoot of the signal which gives rise to a recovery time. The response of preamplifier A to a single electron is shown in different stages in figure 4 (the noise is switched off). The negative tail of the differentiator signal gets longer with a longer integration and differentiation time; this forces us to use time constants as low as possible. We limit ourselves to $\tau_{int} < 50$ ns. We set $\tau_{int} = \tau_{dif}$ in all simulations of the Fastplex-A, so that the shaping time is simply equal to τ_{int} .

The integrator of the Fastplex-B has a much higher integrator decay time, of at least 1 μs , so that the negative tail is smeared out over a much larger time interval. Therefore it will not

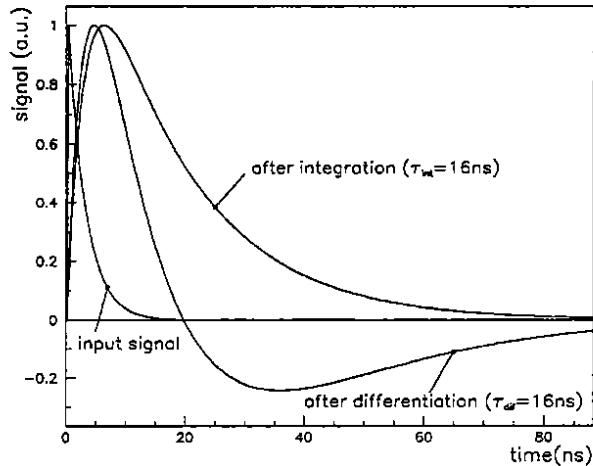


Figure 4: Ideal response of the integrator and differentiator to a test pulse for case A with a shaping time of 16 ns and a rise time of 0 ns. All curves are normalised to 1 separately. Note that even this infinite bandwidth integrator does not come up at once because of the exponential tail of the input signal.

contribute significantly to the signal of later events. The implication of this large integration time is that signals from consequent particles will add up, because it takes the signal from one particle very long to return to zero. This should match the expected rate of 10^5 Hz per strip, so τ_{int} should be less than $10 \mu s$.

With both schemes one should be careful to avoid integrator saturation when a lot of charge is injected at the input. In that case the preamplifier will be dead for many microseconds. As a benchmark event one can take the case that a γ -ray coming from the Transition Radiation Detector in the ATLAS experiment, converts into an e^+e^- pair in the detector. The energy of such a photon can be tens of keV's (it is 6 keV on average). If we want the preamplifier to be able to handle a 30 keV γ , it should not go into saturation at an input charge of 2,000,000 electrons (while the discriminator level is set typically on 10,000 electrons). This sets a scale for the needed dynamic range of the preamplifier.

The bunch crossing scheme of the LHC shows periodical gaps where no beams interact; one can reset the preamplifier on these bunch crossings (by discharging the integrator capacitance). This limits the period of saturation.

4 Optimisation of the frontends for the MSGC

For the Fastplex-A, the Monte Carlo predicts a typical MSGC signal as shown in figure 5. The top left figure shows the signal coming from the anode. Each peak corresponds to the arrival of a cluster to the anode, and the tail of the peak has a decay time of 3 ns, determined by the velocity of the ions that drift away from the anode after the gas amplification process. The figure on the top right is the same signal plus white noise. The signal is integrated with

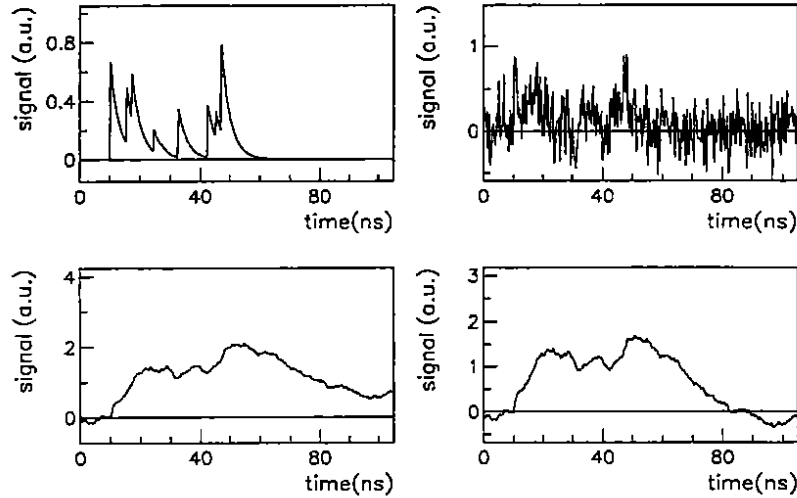


Figure 5: Typical signal on an MSGC anode, before the integrator, after the integrator and after the differentiator.

a time constant $\tau_{int} = 40$ ns, of which the result is shown in the bottom left figure. After the differentiation (with time constant $\tau_{dif} = 40$ ns) the signal looks as in the bottom right figure. The Fastplex-B performs an almost ideal integration of the anode strip signal with a rise time of ~ 20 ns and a very high decay time.

Figure 6 shows the results of the MSGC/frontend simulation. In this figure the signal is kept constant, and the noise is tuned to such a value that the resulting detector efficiency is $98.0\% \pm 0.05\%$. The actual values of the maximal noise are very sensitive to small variations of the electron drift velocity, gas gap thickness and gas mixture, so only comparative conclusions can be drawn. The shaper circuit (case A) turns out to have a strong bias towards relatively high shaping time. With a higher shaping time, the signals from individual clusters are stacked on top of each other giving rise to a higher signal. It also shows a bias towards high rise time. When the rise time is high, the signal slowly approaches the peak value, so it is high over a long period. When the rise time is 0, the signal falls off right from the start. So a longer rise time yields a signal that is maintained longer, thus giving again a better stacking of the different pulses from the primary clusters.

The Fastplex-B shows no significant difference in performance as we vary τ_{int} in the region of interest. This is not surprising because the integrator time constant is higher than the largest time constant in the MSGC in this case. The integration time of the Fastplex-B can be optimised on different criteria than detector efficiency, e.g. on the expected noise level. A small rise time is preferred because the introduction of a rise time results in a smearing of the signal in time so that the subtraction does not yield exactly the collected charge during the past 50 ns.

Note that the scales are very different for the two amplifier schemes. The high shaping time curves have no points at the low edge of the graph, because τ_{int} should be larger than τ_{rise} in equation 1.

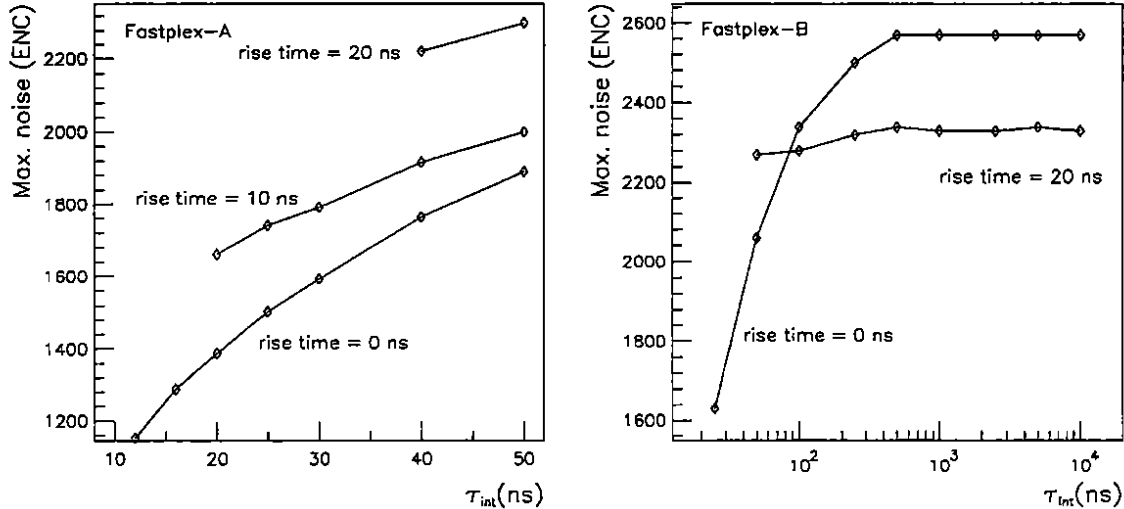


Figure 6: Noise level (in equivalent noise charge) that can be tolerated in the Fastplex-A and Fastplex-B schemes, as a function of the integrator rise and decay time. The shown noise level yields a 98% MSGC efficiency when the discriminator threshold is set to $5 \times$ noise.

5 Conclusions

As compared to signals from silicon strip detectors, the signal from an MSGC has a low amplitude and is highly stochastic; it therefore needs careful handling. The presented simulations show that to achieve a good detector efficiency, it is necessary to integrate the signal of the MSGC strips with a time constant > 40 ns to smooth the spiky signals. One can either use a fast shaping circuit ($\tau \approx 50$ ns) combined with a continuous discriminator, or a very slow integrator ($\tau \approx 1 \mu s$) if the signal difference over a certain time slot is discriminated. The latter scheme seems preferable, because the requirements on the discriminator are much easier to fulfill and the maximum tolerable noise is about 25% higher than with the fast shaping circuit. A disadvantage is the complexity of the Fastplex-B scheme. Of course, there are more parameters involved in a proper comparison of the two than just the detector characteristics discussed in this paper. A detailed simulation or test batch of the frontend electronics is required to find out whether the needed low noise levels can be obtained.

6 Acknowledgements

This work would have been impossible without the input from Ruud Kluit and Paul Rewiersma concerning the behaviour and simulation of the two preamplifier schemes. Ruud Kluit also provided me with figure 3. Bob van Eijk came up with many useful suggestions.

References

- [1] J. Schmitz, NIM A 323 (1992) 638, NIKHEF preprint NIKHEF-H/92-10.
- [2] F. Angholfini et al., CERN 90-10 (1990) 84.